

If such properties are manifest in the cell, they have profound consequences for the structure and dynamics of the microtubule cytoskeleton; they could explain why most of the microtubules in many cell types originate from the centrosome, and why free microtubules, formed for example by removal of depolymerizing drugs, are unstable with respect to centrosomal microtubules<sup>15</sup>.

The *in vitro* experiments demonstrate not only that microtubule assembly off the centrosome is kinetically preferred, but also that centrosomes will be the source of microtubules in the cell in the long term. Although differences in the affinity of the ends of microtubules for tubulin could accentuate the stability of centrosomal microtubules near the steady-state concentration<sup>17</sup>, the properties observed here could operate well below

Received 27 April; accepted 6 September 1984.

1. McIntosh, J. R. *Mod. Cell Biol.* **2**, 115–142 (1983).
2. Wheatley, D. N. *The Centriole: A Central Enigma of Cell Biology* (Elsevier, New York 1982).
3. Calarco-Gillam, P., Siebert, M., Hubble, R., Mitchison, T. & Kirschner, M. *Cell* **35**, 621–629 (1983).
4. Osborn, M. & Weber, K. *Proc. natn. Acad. Sci. U.S.A.* **73**, 867–871 (1976).
5. Brinkley, B. R., Fuller, A. M. & Highfield, D. P. in *Cell Motility* (eds Goldman, R., Pollard, T. & Rosenbaum, J.) 867–871 (Cold Spring Harbor Laboratory, New York, 1976).
6. Frankel, F. R. *Proc. natn. Acad. Sci. U.S.A.* **73**, 2798–2802 (1976).
7. Snyder, J. A. & McIntosh, J. R. *J. Cell Biol.* **67**, 744–760 (1975).
8. Brinkley, B. R. et al. *J. Cell Biol.* **90**, 554–562 (1981).
9. Gould, R. R. & Borisy, G. G. *J. Cell Biol.* **73**, 601–615 (1977).
10. Bergen, L., Kuriyama, R. & Borisy, G. G. *J. Cell Biol.* **84**, 151–159 (1980).
11. Kuriyama, R. *J. Cell Sci.* **66**, 277–295 (1984).
12. Roobol, A., Havercroft, J. C. & Gull, K. *J. Cell Sci.* **55**, 365–381 (1982).
13. Ring, D., Hubble, R., Caput, D. & Kirschner, M. W. in *Microtubules and Microtubule Inhibitors* (eds DeBrabander, M. & DeMey, J.) 297–309 (Elsevier, Amsterdam, 1980).
14. Kuriyama, R. & Borisy, G. G. *J. Cell Biol.* **91**, 822–826 (1981).
15. DeBrabander, M., Geuens, G., DeMey, J. & Joniau, M. in *Microtubules and Microtubule Inhibitors* (eds DeBrabander, M. & DeMey, J.) 255–268 (Elsevier, Amsterdam, 1980).
16. DeBrabander, M., Geuens, G., Nuydens, R., Willebroeck, R. & DeMey, J. *Cell Biol. int. Rep.* **5**, 913–920 (1981).
17. Kirschner, M. W. *J. Cell Biol.* **86**, 330–334 (1980).
18. Hill, T. L. & Kirschner, M. W. *Int. Rev. Cytol.* **84**, 185–234 (1982).
19. Spiegelman, B. M., Lopata, M. & Kirschner, M. W. *Cell* **16**, 239–252 (1979).
20. Sharp, G. A., Osborn, M. & Weber, K. *J. Cell Sci.* **47**, 1–24 (1981).
21. Ring, D., Hubble, R. & Kirschner, M. W. *J. Cell Biol.* **94**, 549–556 (1982).
22. Karsenti, E., Newport, J., Hubble, R. & Kirschner, M. W. *J. Cell Biol.* **98**, 1730–1745 (1984).
23. Mitchison, T. & Kirschner, M. W. *Nature* **312**, 237–242 (1984).
24. Lee, J. C. & Timasheff, S. N. *Biochemistry* **14**, 5183–5187 (1975).
25. Oosawa, F. & Asakura, S. *Thermodynamics of the Polymerization of Protein* (Academic, New York, 1975).
26. Johnson, K. A. & Borisy, G. G. *J. molec. Biol.* **117**, 1–31 (1974).
27. Gaskin, F., Cantor, C. R. & Shelanski, M. L. *J. molec. Biol.* **89**, 737–758 (1974).
28. Jameson, L. & Caplow, M. *J. biol. Chem.* **255**, 2284–2292 (1980).
29. Karr, T. L., Kristoffersson, D. & Purich, D. L. *J. biol. Chem.* **255**, 8567–8572 (1980).
30. Cote, R. H. & Borisy, G. G. *J. molec. Biol.* **150**, 577–602 (1981).
31. Witman, G. B., Cleveland, D. W., Weingarten, M. D. & Kirschner, M. *Proc. natn. Acad. Sci. U.S.A.* **73**, 4070–4074 (1976).
32. Carlier, M.-F. & Pantaloni, D. *Biochemistry* **29**, 1918 (1981).
33. Carlier, M.-F., Hill, T. & Chen, Y.-D. *Proc. natn. Acad. Sci. U.S.A.* **81**, 771 (1984).
34. Blose, S. H., Metzer, D. I. & Feramisco, R. J. *R. J. Cell Biol.* **98**, 847–858 (1984).
35. Weingarten, M. D., Suter, M. S., Littman, D. R. & Kirschner, M. W. *Biochemistry* **13**, 5529–5537 (1974).
36. Terry, B. J. & Purich, D. L. *J. biol. Chem.* **254**, 9469–9476 (1979).
37. Bradford, M. *Analyt. Biochem.* **72**, 248 (1976).

## Dynamic instability of microtubule growth

Tim Mitchison & Marc Kirschner

Department of Biochemistry and Biophysics, University of California at San Francisco, San Francisco, California 94143, USA

We report here that microtubules *in vitro* coexist in growing and shrinking populations which interconvert rather infrequently. This dynamic instability is a general property of microtubules and may be fundamental in explaining cellular microtubule organization.

**MICROTUBULES** are structural filaments in the cytoplasm which are spatially organized and extremely dynamic<sup>1,2</sup>. Recently, considerable effort has been directed towards understanding what produces and stabilizes specific arrangements of microtubules in cells and by what means microtubules can completely reorganize their spatial distribution. In the accompanying paper<sup>3</sup>, we suggest that microtubules nucleated by centrosomes can grow transiently at tubulin concentrations below those at which free microtubules are stable, and that nucleated microtubules coexist as shrinking and growing populations which rarely interconvert. This behaviour is clear only when individual microtubules rather than bulk populations are studied. Here we generalize the results from microtubules nucleated by centrosomes to free microtubules. We examine the detailed kinetics of microtubule assembly to try to account for these unusual dynamic properties.

### Microtubule dilution

The crucial experiment demonstrating unusual dynamics in the preceding paper was that in which the microtubule number and length distributions were measured after centrosomes were regrown initially at a high tubulin concentration, then diluted<sup>3</sup>. The conclusion we drew from that experiment was that some microtubules continued to grow at the same time as others were lost by depolymerization from their distal ends. It seemed likely that this was a general property of microtubules. We therefore

describe here a similar experiment with free microtubules (Fig. 1). Microtubules were first made by spontaneous polymerization in an assembly-promoting buffer. These were then used as seeds and diluted extensively into a tubulin solution well above the steady-state concentration and allowed to elongate for 4 min. The seeds, which were initially 1–2  $\mu\text{m}$  long, elongated to form a sharp distribution with a mean length of 18.3  $\mu\text{m}$  (Fig. 1b). This actively growing population was either fixed immediately or first diluted with warm buffer to just above (15  $\mu\text{M}$ ) or below (7.5  $\mu\text{M}$ ) the steady-state concentration. To assess both the length and number concentration, fixed microtubules were quantitatively sedimented onto grids for electron microscopy. This procedure gave a highly reproducible number concentration (Fig. 1) and when a known polymer mass was used it gave the expected mean length (see, for example, Fig. 4).

The result of this experiment was very similar to that found using centrosome nucleated microtubules<sup>3</sup>, that is, below the steady-state concentration microtubules were found to both grow and shrink (Fig. 1). Above the steady-state concentration, the number of microtubules remained approximately constant (Fig. 1a) and their length increased from 18.3 to 40.2  $\mu\text{m}$  in 10 min, retaining a fairly sharp distribution (Fig. 1d). Below the steady-state concentration, however, the number concentration decreased with time (Fig. 1a), but the mean length still increased from 18.3 to 21.5  $\mu\text{m}$  in 10 min (Fig. 1c). The rate of microtubule

disappearance was similar to that of centrosomal microtubules at the same tubulin concentration, suggesting that a free minus end does not markedly decrease microtubule stability. This experiment demonstrates the coexistence of shrinking and growing populations with free microtubules and the transient growth of microtubules below the steady-state concentration, confirming that the centrosome data were demonstrating a general property of microtubules. The net polymer mass is clearly decreasing at the lower concentration, as the increase in mean length is more than offset by the decrease in number. At the higher concentration, the net polymer mass increases, confirming that the steady-state concentration lies between these concentrations (Fig. 1a). Since no renucleation occurs in this experiment, polymer mass will eventually decrease to zero at the lower concentration. Centrosomes present at the same concentration would, however, continuously renucleate microtubules<sup>3</sup>.

### Microtubule polymerization rates

In order to understand the dynamic processes occurring in the dilution experiment, we sought to determine the quantitative relationship between tubulin concentration and microtubule polymerization and depolymerization rates. A method giving data for plus and minus ends independently was chosen<sup>4</sup>. To determine polymerization rates, flagellar axonemes were mixed with prewarmed tubulin solutions, then fixed at various time intervals and the length of the microtubules polymerized onto each end of the axonemes was determined (the ends of the axoneme are distinguishable in the electron microscope<sup>5</sup>). To determine depolymerization rates, axonemes were first regrown with microtubules, then diluted (Fig. 2). Immunofluorescent visualization was used for higher tubulin concentrations (Fig. 2a) and electron microscopy for lower concentrations (Fig. 2b, c), with equivalent results. For the higher tubulin concentrations, the length increase is linear up to ~20 µm, at which length shear-induced breakage becomes difficult to avoid (Fig. 2a). At the lowest concentrations the mean length rapidly plateaus and only initial rates were used (Fig. 2b). The linear decrease of length with time (Fig. 2c) is consistent with endwise depolymerization.

Figure 3 plots the rate measurements as a function of tubulin concentration. The points on the positive portion of the data, which we refer to as the growing phase, show a linear relationship between growth rate and concentration. This is interpreted in terms of the simple first-order rate equation shown in the legend to Table 1. The values of  $k_T$  for the plus and minus end are quite similar to those derived for microtubule protein<sup>4,6</sup>. As in those studies, the fast-growing end corresponds to the end of the axoneme distal to the cell.

The data cannot be used to derive the  $x$  intercepts very accurately because they are so close to zero, and small changes in the slope produce large changes in their values. The data do not support the assertion that the intercepts for the plus and minus ends are significantly different. Thus, the growing phase

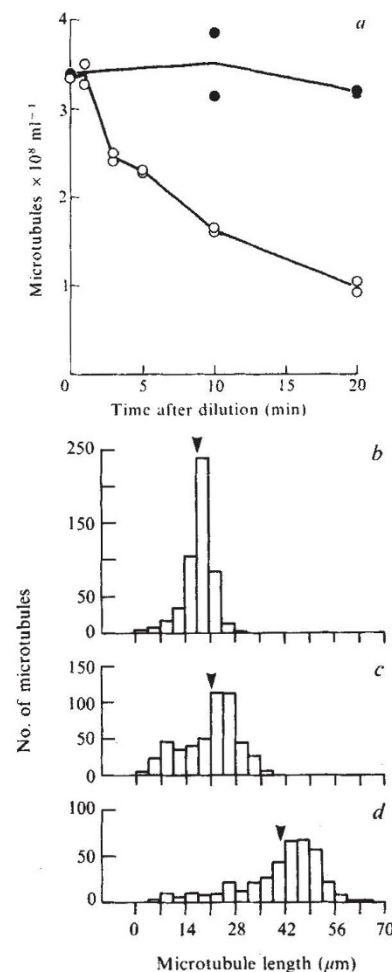


**Fig. 1** Dilution after seeded assembly. *a*, For number concentration, the number of microtubule ends per field was averaged for 16 fields, divided by two and scaled to final number concentration using the geometry of the rotor and the dilution factor. Duplicate grids were made at each time point. Final tubulin concentration: closed circles 15 µM, open circles 7.5 µM. Microtubule lengths were determined by digitizing as in Fig. 6 of ref. 3. *b-d*, Length histograms. *b*, Fixed before dilution (500 measured, mean 18.3 µm, s.d. = 4.0 µm); *c*, 10 min at 7.5 µM (500 measured, mean 21.5 µm, s.d. = 8.6 µm). The mean is significantly increased ( $P < 0.0001$ ) with respect to the starting population. *d*, 10 min at 15 µM (250 measured, mean 40.2 µm, s.d. = 12.0 µm). The arrow points to the mean of each distribution.

**Methods:** Preparation of tubulin, measurement of protein concentration, buffers used and generation of microtubule seeds were as described in Fig. 5 of ref. 3. 1/100 volume of seeds was added to prewarmed tubulin, 25 µM in PB. After 4 min at 37 °C, 10-µl aliquots of the growing microtubules were added to 100 µl of 1% glutaraldehyde in PB' (PB without GTP) at 26 °C or 1 ml of prewarmed tubulin at 15 µM (above steady-state concentration) or 7.5 µM (below steady-state concentration) in PB, and gently mixed. Incubation was continued at 37 °C, and aliquots were fixed at the indicated time intervals. After 3 min in the fixative, the microtubules were diluted with cold PB', and sedimented onto polylysine-coated 150-mesh Parlodion grids in the airfuge EM 90 rotor (Beckman) at 90,000g for 15 min. Grids were previously polylysine-coated by immersion in 1 µg ml<sup>-1</sup> polylysine for 10 min, then dried by aspiration. Grids were dried and shadowed as described in Fig. 4 of ref. 3. Random fields were photographed at a final magnification of  $\times 1,500$ .

**Table 1** Derived rate constants for the kinetics of microtubule assembly

	Plus end	Minus end	Units
Slope	0.135	0.042	µm µM <sup>-1</sup> min <sup>-1</sup>
$k_T$	3.82	1.22	$\times 10^6$ M <sup>-1</sup> s <sup>-1</sup>
$x$ intercept	0.1	0.9	µM
$y$ intercept	-0.013	-0.039	µm min <sup>-1</sup>
$k'_T$	0.37	1.1	s <sup>-1</sup>
Depolymerization rate	-12.0	-7.5	µm min <sup>-1</sup>
$k'_D$	340	212	s <sup>-1</sup>

We assume 1,700 tubulin dimers per µm microtubule. The growth rate ( $J_T$ ) is defined as  $k_T c - k'_T d$ , where  $c$  is the tubulin monomer concentration,  $k_T$  the second-order on-rate constant and  $k'_T$  the extrapolated off-rate constant during polymerization, calculated from  $y$  intercept of Fig. 3.

of microtubules behaves like simple subunit addition to a polymer in equilibrium with its subunits, having the same extremely small critical concentrations for the two ends<sup>7</sup>. In any case, the  $x$  intercepts for both ends are much lower than the steady-state concentration measured on the same tubulin preparation<sup>3</sup>, which was 14 µM. Thus axonemes, like centrosomes, can nucleate

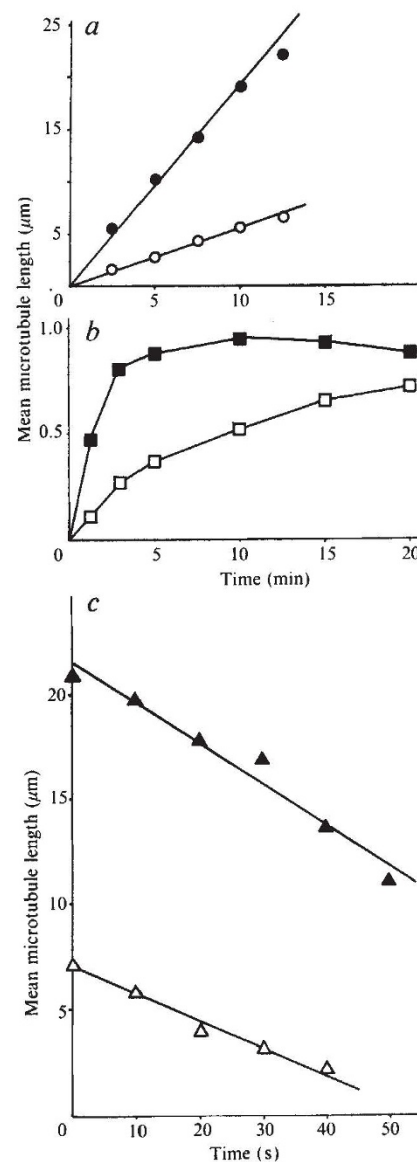
**Fig. 2** Microtubule growth rate off axonemes. *a*, Polymerization at 15  $\mu\text{M}$  tubulin (immunofluorescence). *b*, Polymerization at 3  $\mu\text{M}$  tubulin (electron microscopy). *c*, Depolymerization at 2.5  $\mu\text{M}$  tubulin (electron microscopy).

**Methods:** Axonemes were prepared by washing *Tetrahymena* cells in fresh growth medium, followed by 10 mM PIPES, 1 mM  $\text{MgCl}_2$ , 1 mM  $\text{CaCl}_2$ , pH 7.2 with KOH. Cells were resuspended at 25 °C in the same buffer and dibucaine was added to 0.5 mM<sup>24</sup>. After 5 min the cells shed their axonemes and rounded up. Cell bodies were removed by centrifuging twice at 2,000g for 5 min. The supernatant was made 5 mM in EDTA and 0.5% Triton X-100. Axonemes were pelleted at 25,000g for 20 min at 4 °C and resuspended in 50% (v/v) glycerol, 5 mM PIPES, 0.5 mM EDTA, 1 mM  $\beta$ -mercaptoethanol, pH 7 with KOH at a concentration of  $\sim 10^{10} \text{ ml}^{-1}$ . They could be stored for months at -20 °C in this buffer. Solutions of tubulin in PB were prewarmed to 37 °C for 2 min and axonemes were added to a final concentration of  $10^7 \text{ ml}^{-1}$ . The mixture was incubated at 37 °C and aliquots were fixed as in Fig. 1 at five or six time points. The time course varied from 20 min at the lower to 5 min at the higher concentrations. Fixed regrown axonemes were diluted and sedimented onto polylysine-coated grids in the airfuge as in Fig. 1, or onto polylysine-coated glass coverslips (Fig. 1*b* of ref. 3) except that the spin was for 30 min. Regrown axonemes were then visualized by rotary shadowing and immunofluorescence respectively. For depolymerization experiments, axonemes were pregrown to  $\sim 20 \mu\text{m}$  on the plus and  $\sim 7.5 \mu\text{m}$  on the minus ends. They were then diluted and fixed at 10-s intervals and analysed by electron microscopy. Random axonemes were photographed at  $\times 1,500$  or  $\times 3,000$  in the electron microscope, or at  $\times 250$  in the light microscope and digitized directly from the negatives. At least 100 microtubules from each end were measured at each time point and the time courses were plotted. Rate of microtubule growth was determined by linear regression to the linear portion of the time course, which generally included all points with mean length less than 20  $\mu\text{m}$ , with typical correlation coefficients of  $>0.95$ .

microtubules well below the steady-state concentration, and this can occur on both the plus and minus ends. This also confirms the data of Fig. 1, where microtubules with both plus and minus ends free continued to grow well below the steady-state concentration.

The shrinking phase of Fig. 3 confirms and extends earlier data<sup>8</sup> showing a large break in the bulk polymerization curve (measured by turbidity) where it crossed the *x* axis. For both the plus and minus ends, the observed depolymerization rate is 2-3 orders of magnitude greater than the extrapolated *y* intercept ( $k'_T$ ) from the growing phase of the graph. Thus the off rates during depolymerization, which we call  $k'_D$ , are much larger than the off rates during polymerization,  $k'_T$ . We interpret the difference as being due to the existence of a GTP cap during polymerization, and hence the nomenclature of  $k'_T$  and  $k'_D$  where  $k'_T$  is the off rate of GTP tubulin from a GTP lattice, and  $k'_D$  is the off rate of GDP tubulin from a GDP lattice, in agreement with earlier studies<sup>8</sup>.

It is important to distinguish the kind of data obtained by bulk measurements<sup>8</sup> from the measurement here of individual microtubules. The growing phase data of Fig. 2 is not an aggregate growth rate of both growing and shrinking microtubules because the axoneme template could not depolymerize and thus we only observed net growth. At most of the tubulin concentrations used, microtubules grew continuously during the time course, indicating that the transit of a growing microtubule into the shrinking phase is a relatively rare event. Only at 3 and 4  $\mu\text{M}$  tubulin did phase transitions during the time course become significant. At these concentrations, microtubules depolymerized after transient growth, leading to plateauing of average length and a heterogeneous length distribution. Similarly, during the depolymerization experiments, the tubulin concentrations were sufficiently low that essentially all the microtubules shrank continuously. Thus the two arms of the plot in Fig. 2 cannot be connected. A single shrinking microtubule can transit from the growing phase to the shrinking phase over a wide range of concentrations (Fig. 1; ref. 3).



### Steady-state dynamics

The dynamics at steady state are unclear, because at 14  $\mu\text{M}$  tubulin (where the net polymer mass should be constant) the plus and minus ends should be growing at 1.88 and 0.55  $\mu\text{m min}^{-1}$  respectively, or a total of 2.43  $\mu\text{m min}^{-1}$  for free microtubules. We examined the nature of the steady state by measuring microtubule length and number concentration (Fig. 4). Microtubule polymerization was initiated by seeded assembly and followed by turbidity. After assembly to near steady state the microtubules were sheared. Following a transient decrease in turbidity, the microtubules rapidly attain a plateau in turbidity, corresponding to steady-state assembly (Fig. 4*a*). Sampling during the plateau of turbidity indicated that there is a steady increase in mean microtubule length, while the number concentration decreases steadily. Polymer concentration determined as the product of average length and number is constant (within an experimental error of 10%) and the mean polymer concentration (30  $\mu\text{M}$ ) is in good agreement with that expected from the bulk assembly data in our previous paper (Fig. 5; ref. 3).

The increase of mean length with time demonstrates that most microtubules are indeed growing at the steady-state concentration. Monomer for this growth must be supplied by the depolymerization of shrinking microtubules, and in the absence of renucleation this leads to the observed decline in number concentration. Thus the steady state can be interpreted as being due to the coexistence of two phases, with the majority of microtubules growing slowly balanced by the minority shrinking

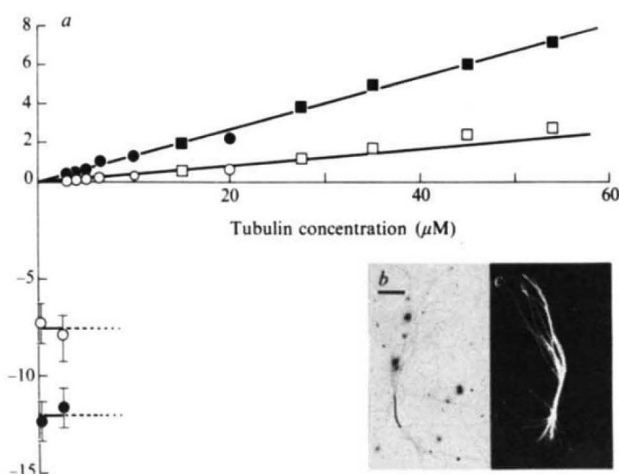


**Fig. 3** *a*, The growth rate of microtubules off axonemes obtained from data of the type in Fig. 2 plotted as a function of tubulin concentration. The closed symbols show data for the plus and the open for the minus ends. Data points plotted as squares were determined by immunofluorescence, and points plotted as circles by electron microscopy and shadowing. The line is a least-squares fit which minimizes relative deviations, that is  $(di/yi)^2$  rather than  $(di)^2$ . All points have similar relative errors thus points at the lower tubulin concentration have smaller absolute errors, so minimizing relative deviation gives the most physically reasonable fit to the data. *b*, Typical regrown axoneme visualized by rotary shadowing and electron microscopy. Scale bar, 4.5  $\mu\text{m}$ . *c*, Typical regrown axoneme visualized by immunofluorescence and printed to the same scale as *b*.

rapidly. The observed length fluctuations are much too large to be explained by random fluctuations of an equilibrium polymer. Using reasonable rate constants, a polymer 15  $\mu\text{m}$  long would take a year to fluctuate to zero by fluctuations at equilibrium<sup>9,10</sup> and the addition of treadmilling would not give the observed rates<sup>11</sup>. End-to-end ligation of microtubules is also unlikely to explain the results, as experiments with pulses of biotin-labelled tubulin have shown only end addition as the mechanism of elongation (manuscript in preparation). The proportion in the two phases can be estimated from Fig. 4, because net growth must balance net disassembly at steady state. Unfortunately, the existence of different kinetics at the two ends complicates the analysis, but if most of the net growth occurs on plus ends at 1.9  $\mu\text{m min}^{-1}$  (the growth rate at 14  $\mu\text{M}$  tubulin dimer) and disassembly occurs off both ends at an average of 9.7  $\mu\text{m min}^{-1}$ , then there will be an average 5.2 growing microtubules for every shrinking one.

If transitions between growing and shrinking phases are very frequent, then little net microtubule elongation (or number loss) would be seen. The observed growth rate (Fig. 4) suggests that such transitions must be rare. A crude way to estimate the transition probabilities is to consider that for microtubules  $\sim 20 \mu\text{m}$  long, the half life for loss in number is  $\sim 20$  min at the plateau in turbidity. Using the kinetic constants described above, such a microtubule would take  $\sim 1.7$  min to depolymerize from the plus end, or  $\sim 2.7$  from the minus end. If  $\sim 20\%$  of the microtubules are depolymerizing at any one time, the half life should be  $\sim 10$  min if they always depolymerize to completion once shrinking is initiated. The observed half life of 20 min may reflect that, on average, half the microtubules depolymerize to completion and half are recapped somewhere during the 20  $\mu\text{m}$  of depolymerization, which represents 34,000 dissociation events. However, determination of the transition rates will require further experiments and detailed modelling.

We favour a model which explains the difference between growing and shrinking microtubules in terms of differences at their ends, in that growing microtubules have GTP-ligated caps whereas shrinking microtubules do not<sup>6</sup>. One observation which supports the idea that growing microtubules are stabilized by their GTP caps is shown in the absorbance traces in Fig. 4.

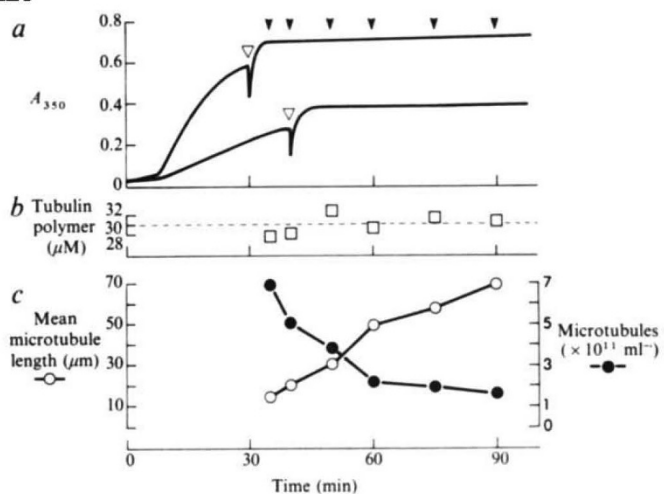


**Fig. 4** Length redistribution at steady state. *a*, Turbidity record: upper trace, total tubulin = 59  $\mu\text{M}$ ; lower trace, total tubulin = 32  $\mu\text{M}$ . Microtubules sampled at times shown by arrows. *b*, The product of mean length and number concentration, expressed as  $\mu\text{M}$  polymer, assuming 1,700 subunits  $\mu\text{m}^{-1}$ . *c*, Number concentration and mean length at the time point denoted by the arrows in *a*, upper trace. The same time scale is used for *a*, *b* and *c*; the points in *c* refer to the samples denoted by closed arrows in *a*. *d*, *e*, *f*, Part of typical immunofluorescence fields. Arrow = 30  $\mu\text{m}$ . Time after shear: *d*, 5 min; *e*, 15 min; *f*, 60 min.

**Methods:** Microtubule seeds were prepared as in Fig. 5 of ref. 1. Tubulin in PB was added to a prewarmed cuvette in a Cary spectrophotometer and incubated throughout at 37 °C. At 8 min, 1/100 volume of seeds was added and the solution mixed. At the time indicated by the open arrow, the growing microtubules were sheared by passing the solution twice through a 22 gauge 1½-inch needle, using a 1-ml syringe which had been prewarmed to 37 °C. From the solution in the upper trace, aliquots were removed for fixation at the times indicated by closed arrows. Aliquots (20  $\mu\text{l}$ ) were added to 2 ml of 1% glutaraldehyde in PB' at 26 °C. After 3 min, the fixed microtubules were further diluted using cold PB'. Wide-mouthed pipette tips and very gentle mixing were used to minimize shear. 100- $\mu\text{l}$  aliquots of diluted microtubules were spun onto 4.5-mm<sup>2</sup> polylysine-coated glass coverslips using the airfuge EM 90 rotor at 90,000g for 15 min. The microtubules were visualized by anti-tubulin immunofluorescence without methanol post-fixation. Microtubules were photographed at  $\times 250$  and  $\times 100$ , and digitized for fluorescent axonemes as in Fig. 2. For the length data, 500 microtubules were measured at each time point. The higher magnification was used for the first three points, and the lower for the last three. For the number data, the number of microtubule ends per field at  $\times 250$  was averaged over 38 fields, divided by two and scaled using the magnification, the geometry of the rotor and the dilution factor.

When the seeded assembly mixture is sheared during the growth phase, there is a large transient decrease in the  $A_{350}$ , indicating considerable microtubule depolymerization. The extent of this drop, which can be up to one-third of the polymer present, depends on the extent of shearing. Merely drawing the solution into a Pasteur pipette has little effect on the  $A_{350}$ . Such a shear-induced depolymerization is not expected from simple theories of polymer polymerization<sup>9</sup>. We interpret this transient depolymerization as being due to the breakage of microtubules, which exposes GDP-ligated subunits at the new ends. These are unstable and start to depolymerize rapidly, a process which continues until new GTP caps can be established.

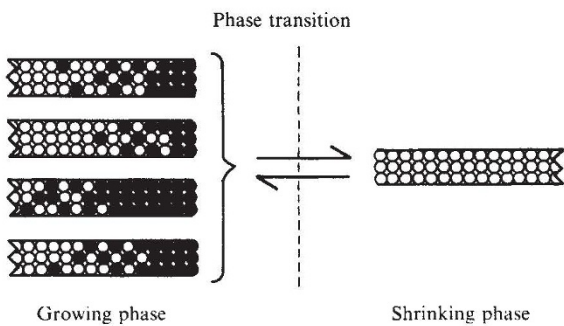


**Fig. 5** Model for microtubule ends exchanging subunits with soluble dimer. The open circles represent tubulin liganded with GDP, and the closed circles represent GTP-tubulin. The growing phase of microtubules is stabilized by a GTP cap. This cap is of fluctuating length, but the average length increases with free tubulin concentration. The shrinking phase has lost this cap. Interconversion between the two phases is relatively rare.

## Microtubule assembly

A new model for microtubule assembly arising from the data presented here and other data<sup>3,8,12</sup> is presented in Fig. 5. The essence of the model is that two distinct phases of microtubules exist which are distinguished by the presence or absence of a GTP-ligated cap, and that the two phases interconvert infrequently. The ends without a cap are unstable at all monomer concentrations tested, that is, GTP subunits will not give net addition to a GDP lattice in the concentration range studied. The GDP lattice thus depolymerizes rapidly, with off rates >100 times faster than the  $y$  intercept extrapolated from the growing phase kinetics (Table 1). The GTP-capped lattice, however, is stabilized, because the off rate of GTP subunits is slower by 2–3 orders of magnitude, so net addition of new GTP subunits occurs down to a very low tubulin concentration. However, the cap only exists because the hydrolysis rate lags slightly behind the polymerization reaction<sup>13</sup>. GTP hydrolysis is a first-order reaction initiated by the conformational change undergone by the subunit once incorporated into the polymer lattice. Thus, once a GTP subunit is incorporated, there is a fixed probability per unit time of hydrolysis occurring. Addition of GTP subunits, however, is a second-order reaction whose rate depends on monomer concentration. At high tubulin concentration there will always be a significant cap of GTP subunits at the growing tip of the polymer. In these circumstances nearly all microtubules will be in the growing phase. However, as the monomer concentration is decreased, the average cap size will decrease, statistical fluctuations in cap size will become important and the probability of GDP subunits becoming exposed on or near the polymer end increases. When this happens, the end subunits are rapidly lost into solution because their affinity for the GDP lattice is low. Once rapid depolymerization is initiated, it continuously exposes fresh GDP subunits at the polymer end and continues until the polymer disappears or a rare event recaps the microtubule and growth restarts. The events that cause a shrinking microtubule to become recapped are not clear. Depolymerization may terminate when encountering remaining GTP in the lattice, and the shrinking end could then become recapped by further addition of GTP-tubulin. The shrinking GDP end may also be capped by binding of GTP tubulin to the GDP end or by direct exchange of GDP for GTP on the terminal subunit.

It is clear, however, that phase transitions in either direction are rare compared with subunit addition in the growing phase or loss in the shrinking phase. Both phase transition probabilities should be quite sensitive to monomer concentration, and perhaps also to the free nucleotide concentrations. An explicit kinetic model incorporating these features has been developed recently<sup>14</sup>. Using plausible rate constants and Monte Carlo calculations, the essential features of persistence of growth and

shrinking (with rare interconversions) have been demonstrated and a general model constructed<sup>15</sup>.

An important question concerns the effect of other components of microtubules, such as microtubule-associated proteins (MAPs), on this dynamic behaviour. It has been suggested<sup>8</sup> that MAP-containing microtubules also have a GTP cap, as they also have a large discontinuity between growing and shrinking kinetics. Some experiments have demonstrated appreciable length fluctuations at steady state<sup>11</sup>. As MAPs bind to the microtubule lattice and stabilize it, they could slow the loss of GDP subunits and increase the probability that a shrinking microtubule would transit into the growing phase. This, in turn, would lower the steady-state concentration. The greater number of transitions at steady state induced by MAPs should tend to damp out the observed length fluctuations. Another factor which would tend to obscure length redistribution at steady state by offsetting the loss of microtubule number is some renucleation of microtubules, which may be strongly promoted by MAPs.

These considerations question the interpretation of isotope uptake experiments by microtubules at steady state as the result of a flux of subunits through the polymer or treadmilling<sup>16,17</sup>. The growing microtubule may behave instead like a simple equilibrium polymer, and extensive isotope uptake may occur through steady-state length redistribution. For microtubules with MAPs, length redistributions (and isotope uptake) would be expected to be less extensive, and in fact the measured isotope uptake is very small for tubulin-containing MAPs<sup>16</sup> compared with purer preparations of tubulin<sup>18</sup>.

Such issues are important because of the question of the relevance of *in vitro* dynamic data with pure tubulin to the living cell. The fast depolymerization rate of microtubules as compared to the extrapolated values from the growing phase holds under various *in vitro* circumstances<sup>8,11,19,20</sup>, and is likely to be true also *in vivo*. This may mean that the primary reason the cell has evolved GTP hydrolysis by tubulin is to have a polymer with built-in instability. Such a polymer could grow rapidly and be stabilized by end interactions, but it could also shrink rapidly, regulated by only small changes in conditions. The ability of microtubules to shrink rapidly may be of importance in reorienting the interphase microtubule array during locomotion or during morphological changes and in the extensive microtubule rearrangements of mitosis<sup>2</sup>. For example, using the off rates for the growing phase, a 20  $\mu\text{m}$  microtubule would take more than 6 h to depolymerize at zero tubulin concentration, but using the off rates for the shrinking phase it would take about 1 min. The importance of the GTP cap in stabilizing growing microtubules raises the possibility that capping proteins may exist in cells and could be required for the long-term stabilization of a microtubule in a cell. Thus the centrosomes may be continually nucleating new microtubules, and only those ends which become capped or become stabilized in some other way such as by inhibition GTP hydrolysis may persist for long periods. A particular example of this could be the capture and capping of centrosomal microtubules by the kinetochore in prometaphase<sup>21,22</sup>.

Various techniques have been used to study the dynamics of microtubules in living cells, and recently the powerful method of introducing fluorescently labelled tubulin molecules into living cells has been exploited. Recent results show that the mitotic spindle is much more dynamic than expected<sup>23</sup> and complete exchange of spindle microtubule and soluble subunits occurs within seconds. Interphase microtubules are considerably more stable but still exchange with soluble subunits within minutes. The dynamic behaviour induced in microtubules by the presence of fluctuating GTP caps provides the only satisfactory *in vitro* explanation for the rapid exchange of spindle microtubules.

We thank T. Hill, M.-P. Carlier and D. Pantaloni for helpful discussion, H. Martinez for the linear regression used in Fig. 2, and Cynthia Cunningham-Hernandez for help in preparing the manuscript. This work was supported by grants from the NIH and the ACS.

Received 27 April; accepted 6 September 1984.

1. Roberts, K. & Hyams, J. *Microtubules* (Academic, London, 1977).
2. McIntosh, J. R. *Mod. Cell Biol.* **2**, 115–142 (1983).
3. Mitchison, T. J. & Kirschner, M. *Nature* **312**, 232–237 (1984).
4. Bergen, L. G. & Borisy, G. G. *J. Cell Biol.* **84**, 141–150 (1980).
5. Allen, C. & Borisy, G. G. *J. molec. Biol.* **90**, 381–402 (1974).
6. Summers, R. & Kirschner, M. W. *J. Cell Biol.* **83**, 205–217 (1979).
7. Hill, T. L. & Kirschner, M. W. *Int. Rev. Cytol.* **84**, 185–234.
8. Carlier, M.-F., Hill, T. L. & Chen, Y.-D. *Proc. natn. Acad. Sci. U.S.A.* **81**, 771–775 (1984).
9. Oosawa, F. & Asakura, S. *Thermodynamics of the Polymerization of Protein* (Academic, New York, 1975).
10. Carlier, M.-F., Pantaloni, D. & Korn, E. D. *J. biol. Chem.* (in the press).
11. Kristofferson, D. & Purich, D. L. *Archs Biochem. Biophys.* **211**, 222–226 (1981).
12. Hill, T. L. & Carlier, M.-F. *Proc. natn. Acad. Sci. U.S.A.* **80**, 7234–7238 (1983).
13. Carlier, M.-F. & Pantaloni, D. *Biochemistry* **20**, 1918–1924 (1981).
14. Hill, T. L. & Chen, Y.-D. *Proc. natn. Acad. Sci. U.S.A.* (in the press).
15. Hill, T. *Proc. natn. Acad. Sci. U.S.A.* (in the press).
16. Margolis, R. L. & Wilson, L. *Cell* **13**, 1–8 (1978).
17. Farrell, K. W. & Jordan, M. A. *J. biol. Chem.* **257**, 3131–3138 (1982).
18. Cote, R. H. & Borisy, G. G. *J. molec. Biol.* **150**, 577–602 (1981).
19. Jameson, L. & Caplow, M. *J. biol. Chem.* **255**, 2284–2292 (1980).
20. Karr, T. L., Kristofferson, D. & Purich, D. L. *J. biol. Chem.* **255**, 8560–8655 (1980).
21. Pickett-Heaps, J., Tippit, D. H. & Porter, K. R. *Cell* **29**, 729–744 (1982).
22. Mitchison, T. J. & Kirschner, M. W. in *Molecular Biology of the Cytoskeleton* (eds Cleveland, D. W., Murphy, D. & Borisy, G. G.) (Cold Spring Harbor Laboratory, New York, in the press).
23. McIntosh, J. & Salmon, E. D. *J. Cell Biol.* (in the press).
24. Thompson, G. A., Baugh, C. C. & Walker, L. F. *J. Cell Biol.* **61**, 253–257 (1974).

## Polyoma virus DNA replication requires an enhancer

Jean de Villiers<sup>\*§</sup>, Walter Schaffner\*, Chiara Tyndall<sup>†§</sup>, Steven Lupton<sup>†§</sup> & Robert Kamen<sup>‡</sup>

\* Institut für Molekularbiologie II der Universität Zürich, Honggerberg CH 8093, Switzerland

† ICRF Laboratories, Lincoln's Inn Fields, London WC2A 3PX, UK

‡ Genetics Institute, 225 Longwood Avenue, Boston, Massachusetts 02115, USA

*Sequences which activate polyoma virus DNA replication are located within a region that also includes the transcriptional enhancer. We demonstrate a cis involvement of enhancers in DNA replication by showing that this region can be replaced by other enhancers, in a position- and orientation-independent manner, and that an immunoglobulin gene enhancer confers tissue-specific replicatory ability.*

UPSTREAM sequences essential for the expression of the early genes of the DNA tumour viruses, simian virus 40 (SV40)<sup>1,2</sup> and polyoma virus<sup>3</sup>, are the archetypes of gene control elements now commonly called transcriptional enhancers. They are *cis*-acting DNA sequences which, when isolated and linked to a variety of genes, dramatically increase expression without increasing template copy number<sup>4–6</sup>.

Enhancers have been identified within the genomes of SV40<sup>4,6</sup>, polyoma virus<sup>5</sup>, bovine papillomavirus<sup>7</sup>, within the long terminal repeats of RNA tumour viruses<sup>8–11</sup> and also within other DNA virus genomes<sup>12–14</sup>. Recently, similar control elements have been shown to be involved in the control of expression of the immunoglobulin genes<sup>15–19</sup> and putative enhancers have been identified in the controlling regions of the human and rat insulin genes and the rat chymotrypsin gene<sup>20</sup>.

Enhancers share a number of properties which together comprise an operational definition. They function over extremely large distances (in some cases, more than several kilobase pairs) and usually in either orientation<sup>4–6</sup>. Transcription is potentiated at both natural and pseudo-promoters and, although activation of transcription from both proximal and distal promoters can be detected, proximal promoters appear to be preferentially affected<sup>21,22</sup>. Enhancers show specificity, ranging from the cell-type preference exhibited by papovavirus and retrovirus enhancers<sup>8,23</sup> to the extreme specificity of the immunoglobulin enhancers for cells of lymphoid origin<sup>15–19</sup>. (For recent reviews see refs 24 and 25.)

The polyoma virus enhancer region has a unique function not yet attributed to other viral or cellular enhancers. It includes *cis* sequence elements essential for viral DNA replication<sup>3,26–28</sup>. Only DNA molecules that have both the polyoma virus origin of replication<sup>27–31</sup> and adjacent (but non-overlapping) sequences

within the enhancer region can replicate in mouse COP-5 cells<sup>3</sup>, despite the fact that these cells constitutively express the viral large-tumour (T) antigen. (This viral early gene product is essential for polyoma virus DNA replication.) We have asked whether the activation of DNA replication is an inherent property of enhancers *per se*, or an independent function of other element(s) within this region of the polyoma virus genome. We have therefore constructed hybrid viral genomes in which the polyoma virus enhancer is replaced by other DNA fragments, to identify heterologous sequences which could substitute for the replicatory activation component.

### Replacement of polyoma virus enhancer

We started with a plasmid recombinant containing the entire 5.3-kilobase (kb) genome of A2 strain polyoma virus (pPy) and deleted, from the regulatory region, the 244-base pair (bp) *Bcl*I to *Pvu*II DNA segment which carries both the transcriptional enhancer<sup>5</sup> and replicatory activator functions<sup>3,27,28</sup> (pPyPBΔ; Fig. 1). Although the origin of DNA replication (ORI) is still present, pPyPBΔ neither expresses its early genes nor replicates even if T antigen is provided (Fig. 1). We then inserted various fragments of DNA from the analogous region of (SV40) at the point of the deletion, because the regulatory region of this closely related virus has distinctive repeated sequence elements (Fig. 1) which are well characterized and have apparently separable functions. We determined the ability of the hybrid DNAs to replicate, independently of the requirement for synthesis of the polyoma virus early gene product T antigen, by assaying DNA replication after transfection of COP-5 cells. These polyoma virus-transformed mouse fibroblast cells constitutively produce the viral early proteins and can replicate plasmids containing only the *cis*-acting elements necessary for viral DNA synthesis<sup>3</sup>. We also assayed DNA replication in mouse 3T6 cells, in which DNA replication is dependent on the ability of the hybrids to express sufficient T antigen and therefore requires both transcriptional enhancer and replicatory activator functions. DNA replication was measured by digestion of extracted DNA with

§ Present addresses: Genetics Institute, 225 Longwood Avenue, Boston, Massachusetts 02115, USA (J.deV.); CSIRO Genetics Research Laboratories, North Ryde, New South Wales, Australia (C.T.); Department of Microbiology, State University of New York, Stony Brook 11794, USA (S.L.).